Probing high-energy electronic excitations in NiO using inelastic neutron scattering

Young-June Kim, A. P. Sorini, C. Stock, T. G. Perring, J. van den Brink, and T. P. Devereaux

Phys. Rev. B **84**, 085132 — Published 29 August 2011

DOI: 10.1103/PhysRevB.84.085132

Probing high-energy electronic excitations using inelastic neutron scattering

Young-June Kim*
Department of Physics, University of Toronto, Toronto, Ontario M5S 1A7, Canada

A. P. Sorini
Stanford Institute for Materials and Energy Science, SLAC National Accelerator Laboratory, Menlo Park, California 94025, USA

C. Stock
NIST Center for Neutron Research, 100 Bureau Drive, Gaithersburg, Maryland 20899, and Indiana University Cyclotron Facility, 2401 Milo B. Sampson Lane, Bloomington, Indiana 47404, USA.

T. G. Perring
ISIS Facility, Rutherford Appleton Laboratory, STFC, Chilton, Didcot, Oxon OX11 0QX, and Department of Physics and Astronomy, University College London, Gower Street, London WC1E 6BT, United Kingdom

J. van den Brink
Institute for Theoretical Solid State Physics, IFW Dresden, 01171 Dresden, Germany

T. P. Devereaux
Stanford Institute for Materials and Energy Science, SLAC National Accelerator Laboratory, Menlo Park, California 94025, USA and Geballe Laboratory for Advanced Materials, Stanford University, Stanford, California 94305, USA

(Dated: August 1, 2011)

High-energy, local multiplet excitations of the d-electrons are revealed in our inelastic neutron scattering measurements on the prototype magnetic insulator NiO. These become allowed by the presence of both non-zero crystal field and spin-orbit coupling. The observed excitations are consistent with optical, x-ray, and EELS measurements of d-d excitations. This experiment serves as a proof of principle that high-energy neutron spectroscopy is a reliable and useful technique for probing electronic excitations in systems with significant crystal field and spin-orbit interactions.

PACS numbers: 78.70.Nx, 71.70.Ch, 71.70.Ej

I. INTRODUCTION

Electrons in strongly correlated systems are characterized by the dual nature of their spatial wave functions; sometimes they are considered localized, but other times delocalized. This dichotomy makes it difficult for traditional band theory to describe physical properties of these scientifically interesting and technologically relevant materials. Often a model based on local interactions, such as a Hubbard Hamiltonian, is used to capture the main physics of these systems, but distilling the numerous interactions present in a condensed matter system into a simple model requires information from experiments. For this reason, various types of electron spectroscopy tools have played significant roles in elucidating various interactions such as crystal field (CF) and spin-orbit (SO) coupling. These include optical, x-ray absorption, photoemission, and electron energy loss spectroscopy (EELS) as well as inelastic x-ray scattering (IXS) in recent years. Here we show that inelastic neutron scattering (INS) can be added to this arsenal of spectroscopic tools for probing *electronic structure* of correlated electron systems.

Neutron spectroscopy has been used to study crystal field splittings in rare-earth insulators[1] and metals[2–5]. With the availability of copious amounts of epithermal neutrons from spallation neutron sources, even inter-multiplet transitions in f-electron systems have been observed with INS[6–9]. Despite earlier theoretical predictions of using INS in studying interband transitions in semiconductors[10], no experimental studies of electronic excitations above 1 eV have been reported to date. Only recently, it was shown that quantitative information above 1 eV can be obtained from direct geometry spectrometers[11]. We note that novel IXS methods have been introduced utilizing either quadrupole transition matrix element[12,13] or resonant enhancement in the soft[14,15] or hard x-ray range[16]. However, such charge-sensitive probes are not ideal for investigating doped Mott insulators, such as cuprate superconductors, because charge carrier contributions dominate the excitation spectrum in the energy range of interest. On the other hand, charge-neutral neutrons do not couple to charge degrees of freedom, and could be very valuable for measuring d-d excitations in such metallic compounds.

In this paper, as a first step towards this goal, we report our observation of localized d-d excitations in NiO using INS. NiO is a prototypical Mott insulator with a large charge-transfer gap of about 4 eV. This material has been studied extensively using various spectroscopic techniques, and its electronic structure is quite well known. In particular, many novel spectroscopic tools have been recently applied to study NiO d-d excitations as a test case, since the NiO d-d excitations are well characterized[17]. For example, spin-polarized EELS[18], soft x-ray resonant inelastic x-ray scattering (RIXS)[14,15], hard x-ray RIXS[16], non-resonant IXS[12], and angle-resolved EELS[19] have all been used to detect d-d excitations in NiO. The benefit of studying NiO is that there is no ambiguity with regard to the identification of d-d excitations, thus allowing us to focus on the mechanism of the spectroscopy.

In our INS investigation of NiO, d-d excitations at 1.0 eV and 1.6 eV have been observed, which is the highest energy d-electron excitation observed with INS to date. These transitions occur via magnetic dipole and higher order scattering operators, respectively, giving strong momentum dependence to their spectral weights. We find that either CF splitting or SO coupling is necessary for the observed transitions, suggesting that one could determine the strengths of these interactions using momentum dependent INS spectrum. We also studied single magnon density of states, which peak up near the zone boundary energy. In contrast to recent soft x-ray RIXS studies, we do not find atomic spin flip scattering at the expected energy range[20]. Our observation thus opens up an exciting new field of electron spectroscopy using INS at quite an opportune time; recently commissioned Spallation Neutron Source will undoubtedly provide an excellent venue for such studies.

II. EXPERIMENTAL METHODS

Total 250 g powder sample of NiO (Alfa Aesar 99 %) was studied on the MAPS and MARI direct geometry time of flight spectrometers located at ISIS (Rutherford Appleton Labs, U.K.). On MAPS, an incident energy of 3 eV was selected by spinning the nimonic chopper at 100 Hz and the "A" Fermi chopper at 600 Hz. On MARI, an incident energy of 500 meV was used with a 50 Hz nimonic and a 600 Hz "A" chopper. All measurements were done at room temperature. Note that the Neel temperature of NiO is well above room temperature.

III. RESULTS AND DISCUSSION

In Fig. 1(a), the intensity map of the excitation spectrum of NiO obtained with E_i=3 eV is plotted. The horizontal axis is momentum transfer (**Q**) and the vertical axis is energy transfer. We have subtracted the high-Q background from the raw data. It is believed that

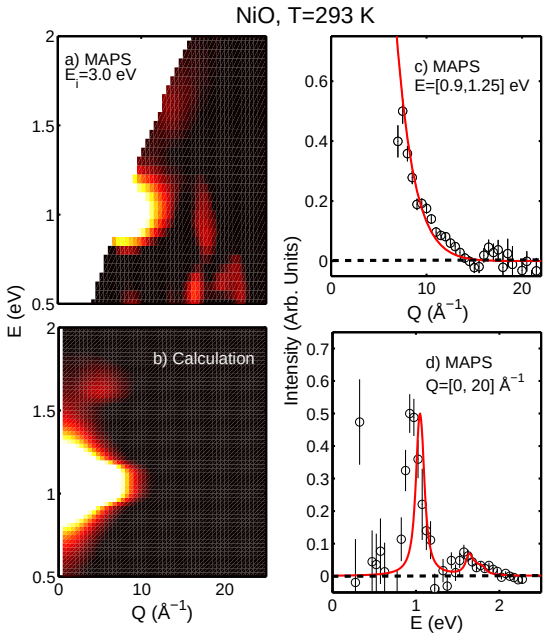

FIG. 1: (Color online) Panel a) is the magnetic intensity map of energy-momentum space obtained on MAPS using incident neutron energy of 3 eV at room temperature. The background intensity due to phonons has been subtracted as discussed in the text. b) illustrates the theoretical calculation discussed in the text. Panels c) and d) illustrate integrated cuts in momentum and energy as noted. The open circles are experimental data and the solid (red) lines are theoretical calculations. As described in the text, the overall amplitude is the only adjustable parameter in the calculation.

the high Q data mostly consist of contributions due to multiple phonons, and the high-Q data were fitted to a form of $A + BQ^2$ and subtracted from the low-Q data as described in Ref.[21]. One can clearly identify a strong spectral feature around the excitation energy of 1 eV, which is more or less dispersionless. The spectral weight on the other hand shows quite strong Q dependence and the intensity falls to the background level around Q=15 Å^{-1}, which is clearly seen in the integrated intensity plot shown in Fig. 1(c). The intensity at higher momentum is due to the background fluctuation. In addition to the 1 eV feature, one can also notice a faint excitation feature around 1.6 eV. This can be more clearly seen in Fig. 1(d), in which we plot the intensity integrated up to Q= 20 Å^{-1} as a function of energy. The well-defined peak centered around 1 eV and additional intensity around 1.6 eV are identified as d-d excitations.

To check if there are hydrogens in the sample, we measured potential hydrogen recoil line[11]. In Fig. 2, we plot the energy and momentum region where hydrogen recoil line is expected (white solid line). As shown in this figure, there is no signature of any hydrogen scattering, eliminating the possibility that the observed excitations come from hydrogen.

In order to understand the scattering mechanism and

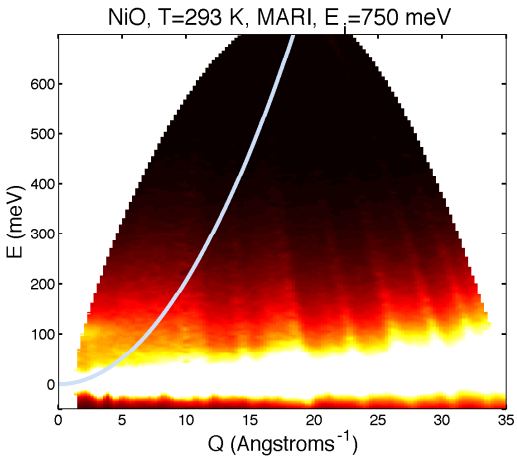

FIG. 2: (Color online) Intensity map of expanded energy and momentum space. The solid white line would correspond to hydrogen recoil.

the observed momentum dependence, we have carried out a cluster calculation. We consider the electronic system to be described by a local model[22] in which the relevant degrees of freedom are the d-electrons of the Ni^{2+} ion in an octahedral ligand field. Our choice of model parameters[14,15] are consistent with previous theory and experiments on d-d excitations of NiO, and were not adjusted to fit our data. The model is parameterized[32] by the $t_{2g} - e_g$ splitting $10Dq = 1.05$ eV, the SO coupling[33] $\xi = 0.051$ eV, and the Racah parameters[32,33] $B = 0.11$ eV and $C = 0.42$ eV. The model includes explicit electron-electron interactions and is solved using the exact-diagonalization method to obtain all the eigenstates and eigenenergies.

The eigenstates and energies are used via Fermi's golden rule to obtain the double differential scattering cross-section for unpolarized neutrons as

$$\frac{d\sigma}{d\Omega d\omega} = \frac{k_f}{k_i}\left(\frac{\gamma_n \mu_N}{c}\right)^2 \sum_f |\mathbf{v}|^2 \delta(E_0 + \omega - E_f) \,, \quad (1)$$

where[23]

$$\mathbf{v} = \frac{1}{Q^2}\mathbf{Q} \times \langle \Psi_f | \sum_i e^{i\mathbf{Q}\cdot\mathbf{r_i}} \left(\mathbf{p_i} + i\mathbf{s_i} \times \mathbf{Q}\right) |\Psi_0\rangle \,, \quad (2)$$

$\mathbf{Q} = \mathbf{k}_i - \mathbf{k}_f$ is the momentum transferred to the electrons, ω is the energy lost by the neutron, and $|\Psi_n\rangle$ and E_n are the states and energies of the electronic system.

The matrix elements in Eq. (2) have a significant dependence on the CF and SO coupling, which can be illustrated by considering the simple limit where $Q \to 0$ (i.e., the magnetic-dipole approximation). In this approximation the allowed excitations are connected to the ground state by the operator $\mathbf{L} + 2\mathbf{S}$, where $\mathbf{L}$ is the total orbital angular momentum and $\mathbf{S}$ is the total spin. For an isolated non-relativistic atom neither $\mathbf{L}$ nor $\mathbf{S}$ can cause inelastic transitions. However, in the presence of a CF it is well known that the diagonal matrix elements of $\mathbf{L}$ are "quenched". The weight that is removed from these diagonal matrix elements effectively appears in the off-diagonal matrix elements; the presence of a CF allows $\mathbf{L}$ to contribute to the inelastic scattering signal. Similarly, the presence of SO coupling allows $\mathbf{S}$ to contribute to the inelastic signal. The magnetic dipole approximation illustrates the importance of CF and SO.

However, due to neutron kinematics, the momentum transfers at energy-loss appropriate for d-d excitation (on the order of eV) can be large compared to the inverse radial size of the electronic orbitals. Thus the magnetic-dipole approximation is not always valid and the full expression, Eq. (2), must be retained. We will see that the dipolar terms give rise to a non-dispersive intra-multiplet peak at $\omega \approx 10Dq$ which dominates the spectrum at low momentum transfer. For higher momentum transfers, non-dipole excitations appear at higher energies (e.g., 1.6 eV) and eventually dominate the relative scattering intensity. The origin of these peaks can be understood roughly from the Tanabe-Sugano diagram[24] for a d^8 system, which describes the change in multiplet energies as a function of CF strength; transitions from the A_1 octahedral symmetry ground state to the higher energy T_2 and T_1 character states give rise to the spectral peaks at ~ 1.0 eV, and ~ 1.6 eV, respectively. The locations of these peaks are slightly shifted and split by SO coupling. The relative intensity of each peak changes with the magnitude of Q as determined by the matrix-elements of Eq. (2).

In Fig. 1(b) we show the theoretical INS intensity map. The energy integral from 0.9 to 1.25 eV over this map, and the momentum integral for $Q < 20$ Å^{-1}, are also shown in Fig. 1(c)-(d) as solid lines. The agreement between theory and experiment is quite good, given that the only adjustable parameter is the overall amplitude. In particular, the momentum dependence shown in Fig. 1(c) suggests that the 1 eV transition occurs via magnetic dipole operator, $\mathbf{L} + 2\mathbf{S}$. The 1.6 eV transition spectral weight is only non-zero in the intermediate Q range, and vanishes both at small and large Q. Since SO coupling in this compound is small, the multiplet splitting due to the SO coupling only shows up as broadening of the 1.6 eV peak.

In addition to the high energy spectrum, we also measured the low energy spin excitation spectrum with E_i=500 meV, as shown in Fig. 3. A clear magnon mode is observed around 100 meV, which is the zone boundary spin wave energy. The assignment of this feature is unambiguous in INS. Earlier neutron scattering studies of spin wave dispersion reported that the zone boundary magnon energy is 117 meV[25,26]. In Fig. 3(b), we plot the intensity as a function of Q. The solid line is the magnetic form factor from the spin angular momentum contribution as tabulated in Ref.[27]. In Fig. 3(c), the low-Q intensity (integrated up to 5 Å^{-1}.) is plotted as a function of energy transfer. Since we are using a powder sample, this integration is a quick method to obtain the

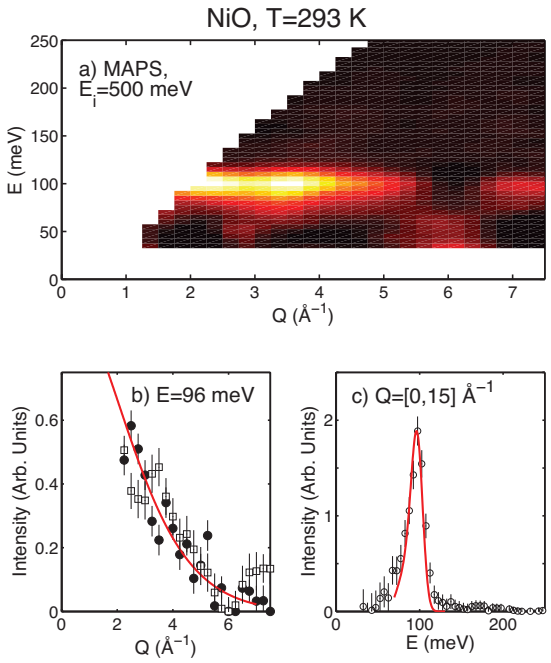

FIG. 3: (Color online) Panel a) illustrates a false contour plot taken on MAPS with the E_i=500 meV. b) the intensity of the peak at 96 meV as a function of momentum transfer. The solid and open points are from MARI (E_i=750 meV) and MAPS (E_i=500 meV) respectively. The solid red line is the free ion Ni^{2+} form factor. c) The momentum integrated scattering and solid line is the calculated density of states from Ref.[25].

magnon density of states. We compare this result with the calculated magnon density of states from Hutchings and Samuelsen[25], which agrees very well.

These lower-energy results shed light on understanding excitations observed with different spectroscopic techniques in the energy range of 100-200 meV. As shown in Fig. 3, no significant scattering intensity is observed above the one magnon band up to 250 meV. This should be compared with earlier photon spectroscopy investigation. In optical spectroscopy studies[28], a two-magnon mode at 193 meV was observed with Raman scattering, while an infrared absorption mode due to two-magnon plus phonon was observed at 250 meV. In a recent Ni L_3-edge RIXS study[20], the excitations at 95 meV and 190 meV were associated with transitions between atomic levels split by an exchange field[29]. We note that "two-magnon" excitations in neutron scattering usually refers to longitudinal spin fluctuations, which usually forms a broad continuum and has very small intensity[30]. The apparent lack of excitations around 190 meV in our INS data clearly illustrates the difference between the "two-magnon" excitations detected with photon spectroscopy and neutron spectroscopy. Further theoretical calculation is necessary to address this issue quantitatively[31].

IV. SUMMARY AND CONCLUSIONS

In summary, we observed d-d excitations of 1 eV and 1.6 eV in NiO using inelastic neutron scattering. Such local multiplet transitions are allowed in the magnetic dipole and higher order channel due to the presence of non-zero crystal field and spin-orbit coupling. The excitation energy matches well with previous experiments, and the momentum dependence of the spectral weight could be well described by the cluster model calculation. Our observation illustrates that inelastic neutron scattering at high energies is a reliable and useful technique for probing electronic excitations in materials with significant crystal field and spin-orbit coupling.

Acknowledgments

We would like to thank K. Plumb for valuable discussions. Y.-J. K. was supported by Natural Sciences and Engineering Research Council of Canada, Canadian Foundation for Innovation, and Ontario Ministry of Research and Innovation. A.P.S. and T.P.D. are supported by the U.S. Department of Energy under Contracts No. DE-AC02-76SF00515 and No. DE-FG02-08ER46540 (CMSN).

* Electronic address: yjkim@physics.utoronto.ca

[1] B. N. Brockhouse, L. N. Becka, K. R. Rao, R. N. Sinclair, and A. D. B. Woods, J. Phys. Soc. Japan **17, Suppl. B-III**, 63 (1962).
[2] B. Rainford, K. C. Turberfield, G. Busch, and O. Vogt, Journal of Physics C: Solid State Physics **1**, 679 (1968).
[3] K. C. Turberfield, L. Passell, R. J. Birgeneau, and E. Bucher, Phys. Rev. Lett. **25**, 752 (1970).
[4] R. J. Birgeneau, E. Bucher, L. Passell, and K. C. Turberfield, Phys. Rev. B **4**, 718 (1971).
[5] P. Fulde and M. Loewenhaupt, Adv. Phys. **34**, 589 (1985).
[6] S. M. Shapiro, R. J. Birgeneau, and E. Bucher, Phys. Rev. Lett. **34**, 470 (1975).
[7] A. D. Taylor, R. Osborn, K. A. McEwen, W. G. Stirling, Z. A. Bowden, W. G. Williams, E. Balcar, and S. W. Lovesey, Phys. Rev. Lett. **61**, 1309 (1988).
[8] R. Osborn, K. McEwen, E. Goremychkin, and A. Taylor, Physica B **163**, 37 (1990).
[9] R. Osborn, S. W. Lovesey, A. D. Taylor, and E. Balcar, in *Handbook on the Physics and Chemistry of Rare Earths*, edited by K. A. Gschneidner, Jr. and L. Eyring (North-Holland, Amsterdam, 1991), Vol. 14, p. 1.
[10] J. F. Cooke and J. A. Blackman, Phys. Rev. B **26**, 4410 (1982).
[11] C. Stock, R. A. Cowley, J. W. Taylor, and S. M. Bennington, Phys. Rev. B **81**, 024303 (2010).
[12] B. C. Larson, W. Ku, J. Z. Tischler, C.-C. Lee, O. D. Restrepo, A. G. Eguiluz, P. Zschack, and K. D. Finkelstein,

Phys. Rev. Lett. **99**, 026401 (2007).
[13] M. W. Haverkort, A. Tanaka, L. H. Tjeng, and G. A. Sawatzky, Phys. Rev. Lett. **99**, 257401 (2007).
[14] G. Ghiringhelli, M. Matsubara, C. Dallera, F. Fracassi, R. Gusmeroli, A. Piazzalunga, A. Tagliaferri, N. B. Brookes, A. Kotani, and L. Braicovich, Journal of Physics: Condensed Matter **17**, 5397 (2005).
[15] S. G. Chiuzbăian, G. Ghiringhelli, C. Dallera, M. Grioni, P. Amann, X. Wang, L. Braicovich, and L. Patthey, Phys. Rev. Lett. **95**, 197402 (2005).
[16] S. Huotari, T. Pylkkanen, G. Vanko, V. R, P. Glatzel, and G. Monaco, Phys. Rev. B **78**, 041102 (2008).
[17] R. Newman and R. M. Chrenko, Phys. Rev. **114**, 1507 (1959).
[18] B. Fromme, C. Koch, R. Deussen, and E. Kisker, Phys. Rev. Lett. **75**, 693 (1995).
[19] F. Müller and S. Hüfner, Phys. Rev. B **78**, 085438 (2008).
[20] G. Ghiringhelli, A. Piazzalunga, C. Dallera, T. Schmitt, V. N. Strocov, J. Schlappa, L. Patthey, X. Wang, H. Berger, and M. Grioni, Phys. Rev. Lett. **102**, 027401 (2009).
[21] C. Stock, L. C. Chapon, O. Adamopoulos, A. Lappas, M. Giot, J. W. Taylor, M. A. Green, C. M. Brown, and P. G. Radaelli, Phys. Rev. Lett. **103**, 077202 (2009).
[22] F. de Groot and A. Kotani, *Core Level Spectropscopy of Solids* (CRC Press, Boca Raton, 2008), pp. 119–121.
[23] E. Balcar and S. W. Lovesey, *Theory of Magnetic Neutron and Photon Scattering* (OUP, Oxford, 1989).
[24] Y. Tanabe and S. Sugano, J. Phys. Soc. Jpn. **9**, 766 (1954).
[25] M. T. Hutchings and E. J. Samuelsen, Phys. Rev. B **6**, 3447 (1972).
[26] M. T. Hutchings and E. J. Samuelsen, Solid State Commun. **9**, 1011 (1971).
[27] P. J. Brown, in *International tables for crystallography, v. C. Mathematical, physical and chemical tables*, edited by A. Wilson (D. Reidel Pub. Co., Dordrecht, Holland, 1995), pp. 391–399.
[28] R. E. Dietz, G. I. Parisot, and A. E. Meixner, Phys. Rev. B **4**, 2302 (1971).
[29] F. M. F. de Groot, P. Kuiper, and G. A. Sawatzky, Phys. Rev. B **57**, 14584 (1998).
[30] T. Huberman, R. Coldea, R. A. Cowley, D. A. Tennant, R. L. Leheny, R. J. Christianson, and C. D. Frost, Phys. Rev. B **72**, 014413 (2005).
[31] C.-C. Chen, C. J. Jia, A. F. Kemper, R. R. P. Singh, and T. P. Devereaux, Phys. Rev. Lett. **106**, 067002 (2011).
[32] J. S. Griffith, *The Theory of Transition Metal Ions* (CUP, Cambridge, UK, 1961).
[33] R. D. Cowan, *The Theory of Atomic Structure and Spectra* (University of California Press, Berkeley, 1981).